




Isospectral and square-root Cholesky photonic lattices

P. I. Martínez Berumen * and B. M. Rodríguez-Lara †

Tecnológico de Monterrey, Escuela de Ingeniería y Ciencias, Avenida Eugenio Garza Sada 2501, Monterrey, N.L., 64849, Mexico

 (Received 20 May 2020; accepted 28 September 2020; published 22 October 2020)

Cholesky factorization provides photonic lattices that are the isospectral partners or the square root of other arrays of coupled waveguides. The procedure is similar to that used in supersymmetric quantum mechanics. However, Cholesky decomposition requires initial positive-definite mode-coupling matrices and the resulting supersymmetry is always broken. That is, the isospectral partner has the same range as that of the initial mode-coupling matrix. It is possible to force a decomposition where the range of the partner is reduced but the characteristic supersymmetric intertwining is lost. As an example, we construct a Cholesky isospectral partner and the square root of a waveguide necklace with cyclic symmetry. We use experimental parameters from the telecommunication C band to construct a finite-element model of these Cholesky photonic lattices to good agreement with our analytic prediction.

DOI: [10.1103/PhysRevA.102.043521](https://doi.org/10.1103/PhysRevA.102.043521)

I. INTRODUCTION

The optical analogy of supersymmetric quantum mechanics (SUSY QM) can be traced back to planar waveguides with an elliptic transversal index profile, where the paraxial approximation provides exact SUSY that breaks for nonparaxial fields [1]. Theoretical curiosity gave place to practical applications with the proposal to use SUSY as a tool for the synthesis of optical structures with particular spectral properties in both bulk and discrete optics [2]. In particular, discrete SUSY photonic lattices may serve in optical communications providing multiplexing schemes [3], mode selection [4], optical intersections [5], Bragg grating filters [6], and mode conversion [7,8], to mention a few examples.

The analogy between the wave equation in the paraxial approximation and the Schrödinger equation allows using standard SUSY QM techniques [9], for example, the Darboux transformation of an optical analog to the Hamiltonian $\hat{H}_1 = -(\hbar^2/2m)(d^2/dx^2) + V_1(x) \equiv \hat{A}\hat{A}^\dagger$ to produce an isospectral partner $\hat{H}_2 = -(\hbar^2/2m)(d^2/dx^2) + V_2(x) \equiv \hat{A}^\dagger\hat{A}$. The effective potentials, proportional to the square of refractive index distributions, are related by a superpotential $W(x)$ that solves Riccati equations $V_1(x) = W^2(x) + (\hbar/\sqrt{2m})W'(x)$, $V_2(x) = W^2(x) - (\hbar/\sqrt{2m})W'(x)$, and allows writing the operators $\hat{A} = -(\hbar/2m)(d^2/dx^2) + W(x)$ and $\hat{A}^\dagger = (\hbar/2m)(d^2/dx^2) + W(x)$. This technique is commonly used to design optical systems [6,10]. The analysis is done for an infinite-dimension device that is cut off to a size large enough to see the desired effects in real world applications [2–8,10–16]. On the other hand, it is possible to work with finite-dimensional optical devices and show SUSY with different Witten indices by the addition of \mathcal{PT} symmetry [17]. This has inspired the use of optical lattices and their superpartners to design laser arrays

by the addition of gain and loss following different seeding patterns [12–15,18]. Factorization methods from linear algebra are a practical tool in some of these designs [2,3,7,13–15,18,19].

Our research program advocates the use of abstract symmetries to optimize optical design processes [20]. For example, it is possible to construct SUSY photonic lattices partners that have a semi-infinite dimension using the special unitary algebra $su(1, 1)$ as the underlying symmetry [16,21]. While the closed-form analysis is done in infinite dimensions, large arrays of the order of hundreds of elements follow the analytic predictions. It is also possible to construct SUSY partners for finite-dimensional lattices using, for example, an underlying $su(2)$ symmetry [22]. In discrete optical systems described by coupled-mode theory, Cholesky factorization is a helpful linear algebra tool to decompose the mode-coupling matrix [2,7,19], and then use the particular modes as seeds to design, for example, parity anomaly lasers [13].

In the following, we review Cholesky factorization of positive-definite real symmetric matrices and its relation with the properties expected from standard SUSY QM with a Witten index two [23–27]. We show that this approach provides us with isospectral and square-root partners with an underlying symmetry defined by the supersymmetric algebra [28] (Sec. II). Then, we use waveguide necklaces with an underlying cyclic group Z_N symmetry as the original partner to construct practical examples of broken SUSY partners. In particular, we provide an analytic isospectral partner for a two-waveguide necklace and a square-root partner for a four-waveguide necklace. We compare our theoretic predictions with a numeric finite-element modeling simulation based on experimental parameters from laser-inscribed realizations (Sec. III). In Sec. IV, we discuss the fact that it is possible to force a pseudo-zero-energy mode. The result is a viable optical system that shows the spectral characteristics but is not exact SUSY as the intertwining relation breaks. We close with a summary and our conclusion in Sec. V.

*A00818058@itesm.mx

†bmlara@tec.mx

II. CHOLESKY LATTICES

Coupled-mode theory simplifies the description of electromagnetic field modes propagating through arrays of coupled waveguides [29]. Instead of describing polarized localized spatial field modes at each waveguide, $E_j = \mathcal{E}_j \Psi(\mathbf{r}) \hat{\mathbf{e}}$, it provides an approximation,

$$i\partial_z \mathbf{E} = \mathbf{M} \mathbf{E}, \quad (1)$$

for the dynamics of the complex field amplitudes summarized in the amplitude vector with a j th component $\mathbf{E}_j = \mathcal{E}_j$. The diagonal terms of the mode-coupling matrix provide information about the propagation constant of localized field modes, $M_{ii} = \beta_i > 0$, and the off-diagonal ones of the coupling strength between modes localized in pairs of waveguides, $M_{ij} = M_{ji} = g_{ij} > 0$. Usually, nearest neighbors are the strongest coupled and a standard approximation is to neglect high-order neighbors. In the optical and telecommunication regimes, the propagation constants are at least three orders of magnitude larger than the coupling strengths. Under these circumstances, the mode-coupling matrix is positive definite.

Cholesky factorization decomposes a positive-definite Hermitian matrix,

$$\mathbf{M} = \mathbf{A} \mathbf{A}^\dagger, \quad (2)$$

into the product of a positive-definite lower triangular matrix \mathbf{A} and its conjugate transpose \mathbf{A}^\dagger ; herein, we call these Cholesky matrices. This suggests the use of SUSY QM ideas to construct the isospectral partner of our mode-coupling matrix. Let us define a new pair of extended Cholesky matrices,

$$\mathbf{Q} = \begin{pmatrix} 0 & 1 \\ 0 & 0 \end{pmatrix} \otimes \mathbf{A} \quad \text{and} \quad \mathbf{Q}^\dagger = \begin{pmatrix} 0 & 0 \\ 1 & 0 \end{pmatrix} \otimes \mathbf{A}^\dagger, \quad (3)$$

that are nilpotent by construction, $\mathbf{Q}^2 = \mathbf{Q}^{\dagger 2} = 0$. In consequence, these two matrices commute,

$$[\mathbf{H}, \mathbf{Q}] = [\mathbf{H}, \mathbf{Q}^\dagger] = 0, \quad (4)$$

with a new block-diagonal matrix,

$$\mathbf{H} = \mathbf{Q} \mathbf{Q}^\dagger + \mathbf{Q}^\dagger \mathbf{Q} = \begin{pmatrix} \mathbf{M} & 0 \\ 0 & \mathbf{P} \end{pmatrix}, \quad (5)$$

that has our mode-coupling matrix \mathbf{M} and a new matrix,

$$\mathbf{P} = \mathbf{A}^\dagger \mathbf{A}, \quad (6)$$

that we call its partner, in the main diagonal. It is straightforward to show a matrix intertwining relation,

$$\mathbf{Q}^\dagger \mathbf{H}_M = \mathbf{H}_P \mathbf{Q}^\dagger, \quad (7)$$

where we define expanded mode-coupling and partner matrices, $\mathbf{H}_M = \mathbf{Q} \mathbf{Q}^\dagger$ and $\mathbf{H}_P = \mathbf{Q}^\dagger \mathbf{Q}$, in that order. It is possible to construct the normal modes of the extended partner matrix starting from those of the extended coupling matrix,

$$\mathbf{H}_M \mathbf{m}_j = \mu_j \mathbf{m}_j, \quad (8)$$

and multiply them by \mathbf{Q}^\dagger from the left,

$$\mathbf{Q}^\dagger \mathbf{H}_M \mathbf{m}_j = \mu_j \mathbf{Q}^\dagger \mathbf{m}_j, \quad (9)$$

to use the matrix intertwining relation,

$$\mathbf{H}_P \mathbf{Q}^\dagger \mathbf{m}_j = \mu_j \mathbf{Q}^\dagger \mathbf{m}_j, \quad (10)$$

and obtain the extended partner matrix normal modes,

$$\mathbf{H}_P \mathbf{p}_j = \mu_j \mathbf{p}_j, \quad \text{with} \quad \mathbf{p}_j = \mathbf{Q}^\dagger \mathbf{m}_j. \quad (11)$$

The extended matrix has identical spectrum as long as $\mathbf{Q}^\dagger \mathbf{m}_j \neq 0$. Cholesky factorization provides positive-definite extended matrices. In consequence, this method always provides isospectral partners.

We keep borrowing from SUSY QM and construct a pair of Hermitian matrices,

$$\mathbf{H}_X = \mathbf{Q}^\dagger + \mathbf{Q}, \quad \text{and} \quad \mathbf{H}_Y = -i(\mathbf{Q}^\dagger - \mathbf{Q}), \quad (12)$$

that are the square root of the previous diagonal matrix,

$$\mathbf{H}_X^2 = \mathbf{H}_Y^2 = \mathbf{H}, \quad (13)$$

and share normal modes with it,

$$\mathbf{H}_X \mathbf{x}_j = x_j \mathbf{x}_j, \quad \text{and} \quad \mathbf{H}_Y \mathbf{x}_j = x_j^2 \mathbf{x}_j. \quad (14)$$

These modes are doubly degenerate for the diagonal matrix \mathbf{H} as we can define some general mode,

$$\mathbf{v}_j = \mathbf{H}_Y \mathbf{x}_j, \quad (15)$$

and realize that it is also an eigenvalue of the new matrix,

$$\mathbf{H}_X \mathbf{v}_j = -x_j \mathbf{v}_j, \quad (16)$$

where we used the fact that $\{\mathbf{H}_X, \mathbf{H}_Y\} = \mathbf{H}_X \mathbf{H}_Y + \mathbf{H}_Y \mathbf{H}_X = 0$ leads to the relation $\mathbf{H}_X \mathbf{H}_Y = -\mathbf{H}_Y \mathbf{H}_X$. This eigenvalue equation implies that the spectrum of the block-diagonal matrix \mathbf{H} is doubly degenerate and the spectrum of the block-antidiagonal matrix \mathbf{H}_X has paired eigenvalues $\pm x_j$.

Before moving forward to practical examples, we want to stress that the Cholesky decomposition of Hermitian positive-definite mode-coupling matrices \mathbf{M} provides isospectral partners \mathbf{P} . Thus, the block-diagonal matrix \mathbf{H} has a doubly degenerate spectrum and its square-root matrix \mathbf{H}_X has a paired spectrum. Owing to the fact that the mode-coupling matrix diagonal terms are larger than the off-diagonal terms, we can find a sequence of isospectral partners and square-root matrices just by decomposing,

$$\mathbf{M} = \alpha \mathbf{1} + \mathbf{M}_\alpha. \quad (17)$$

As long as the new effective mode-coupling matrix \mathbf{M}_α is positive definite, we can find isospectral and square-root matrices of \mathbf{M}_α for each parameter α that might or might not be experimentally viable.

III. WAVEGUIDE NECKLACES

In order to provide a working example, we study a so-called waveguide necklace composed by N identical cores equidistantly distributed on a circle of radius r . The spectrum of these arrays is straightforward to calculate including couplings of all orders [30]. We assume a weakly coupled necklace described by the mode-coupling matrix,

$$[\mathbf{M}(\beta_0, g)]_{i,j} = \beta_0 \delta_{i,j} + g(\delta_{i,j+1} + \delta_{i+1,j}), \quad (18)$$

where the propagation constant of the localized modes at each waveguide is β_0 , the coupling strength between first neighbors

is g , and the addition in Kronecker delta subindices is modulus N such that $N + k \equiv \text{mod}_N(N + k) = k$. The spectrum is positive definite,

$$\beta_j = \beta_0 + g \begin{cases} (-1)^{j-1}, & N = 2, \\ 2 \cos \frac{(j-1)\pi}{m}, & N = 2m, \\ 2 \cos \frac{2(j-1)\pi}{2m+1}, & N = 2m + 1, \end{cases} \quad (19)$$

and has m duplicated elements with one (two) nonduplicated values for odd (even) dimension. The spectrum elements with a minimum value,

$$\beta_{\min} = \beta_0 - g \begin{cases} 1, & N = 2, \\ 2, & N = 2m, \\ 2 \cos \frac{2m}{2m+1}\pi, & N = 2m + 1, \end{cases} \quad (20)$$

suggest the decomposition,

$$\mathbf{M}(\beta_0, g) = (\beta_0 - \epsilon)\mathbf{1} + \mathbf{M}(\epsilon, g), \quad \epsilon > \beta_0 - \beta_{\min}, \quad (21)$$

to construct any given Cholesky isospectral and square-root matrices by focusing on just the positive-definite reduced coupled-mode matrix $\mathbf{M}(\epsilon, g)$.

A. Isospectral partner example

Let us start from the simplest analytically solvable example, two waveguides with a reduced coupled-mode matrix,

$$\mathbf{M}(\epsilon, g) = \begin{pmatrix} \epsilon & g \\ g & \epsilon \end{pmatrix}, \quad \epsilon > g, \quad (22)$$

with eigenvalues

$$\lambda_1 = \epsilon - g \quad \text{and} \quad \lambda_2 = \epsilon + g, \quad (23)$$

and Cholesky decomposition

$$\mathbf{A} = \begin{pmatrix} \sqrt{\epsilon} & 0 \\ \frac{g}{\sqrt{\epsilon}} & \sqrt{\frac{\epsilon^2 - g^2}{\epsilon}} \end{pmatrix}, \quad (24)$$

yielding a partner mode-coupling matrix,

$$\mathbf{P}(\epsilon, g) = \begin{pmatrix} \frac{\epsilon^2 + g^2}{\epsilon} & g\sqrt{\frac{\epsilon^2 - g^2}{\epsilon^2}} \\ g\sqrt{\frac{\epsilon^2 - g^2}{\epsilon^2}} & \frac{\epsilon^2 - g^2}{\epsilon} \end{pmatrix}, \quad (25)$$

isospectral to the original matrix $\mathbf{M}(\epsilon, g)$ with a different experimental arrangement. The diagonal elements point to a $2g^2/\epsilon$ difference between the propagation constants of the localized modes in the waveguides and their coupling constant is smaller than the original partner. We introduce the propagation constant difference into our design by controlling the transverse area or the refractive index of the waveguide cores and the smaller coupling constant by separating the waveguides.

As a practical example, we use two cylindrical waveguides of radius $r = 4.5 \mu\text{m}$, with core and cladding refractive indices $n_{\text{co}} = 1.4479$ and $n_{\text{cl}} = 1.444$, respectively, and separation between core centers of $3r$. In the telecom C band, $\lambda = 1550 \text{ nm}$, these lead to localized mode propagation constants and coupling strength $\beta = 5.87642 \times 10^6 \text{ rad/m}$ and $g = 416.193 \text{ rad/m}$, in that order. We propose a value of $\epsilon = 1.1g$ to construct a partner mode-coupling matrix. This

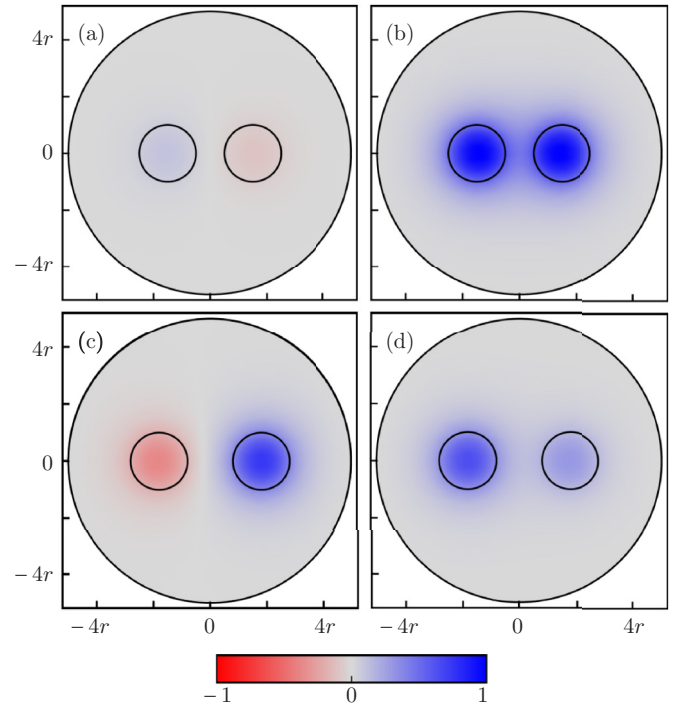


FIG. 1. Finite-element modeling of normal modes (a), (b) of a two-waveguide necklace and (c), (d) its isospectral partner. The propagation constant is (a)–(c) $\beta_a = 5.87648 \times 10^6 \text{ rad/m}$ for asymmetric and (b)–(d) $\beta_s = 5.87731 \times 10^6 \text{ rad/m}$ for symmetric modes; see text for more details.

implies a difference between the effective localized propagation constants of $\Delta\beta = 756.715 \text{ rad/m}$ and coupling strength $g = 173.385 \text{ rad/m}$. The difference in propagation constants corresponds to an increment of $7.496 \times 10^{-3}\%$ in the refractive index of one of the waveguides that is reasonable with changes in the writing speed for laser-inscribed setups [31–36]. The new coupling strength implies a separation of $3.606060r$ between the waveguide cores (Fig. 1). The analytic effective propagation constants for the asymmetric and symmetric normal modes are $\beta_a = 5.876003 \times 10^6 \text{ rad/m}$ and $\beta_s = 5.876835 \times 10^6 \text{ rad/m}$ and the finite-element model simulation provides $\beta_a = 5.859239 \times 10^6 \text{ rad/m}$ and $\beta_s = 5.860186 \times 10^6 \text{ rad/m}$ for \mathbf{M} , and $\beta_a = 5.859626 \times 10^6 \text{ rad/m}$ and $\beta_s = 5.860143 \times 10^6 \text{ rad/m}$ for \mathbf{P} , that are within 0.3% of the predicted values.

B. Square-root example

A waveguide necklace with four elements $N = 4$ described by the following real symmetric, positive-definite reduced coupled-mode matrix,

$$\mathbf{M}(\epsilon, g) = \begin{pmatrix} \epsilon & g & 0 & g \\ g & \epsilon & g & 0 \\ 0 & g & \epsilon & g \\ g & 0 & g & \epsilon \end{pmatrix}, \quad (26)$$

with the restriction $\epsilon > 2g$ has a real positive spectrum $\{\epsilon - 2g, \epsilon, \epsilon, \epsilon + 2g\}$ with corresponding orthonormal modes $\mathbf{m}_1 = (-1, 1, -1, 1)/2$, $\mathbf{m}_2 = (0, -1, 0, 1)/\sqrt{2}$, $\mathbf{m}_3 = (-1, 0, 1, 0)/\sqrt{2}$, and $\mathbf{m}_4 = (1, 1, 1, 1)/2$ independent

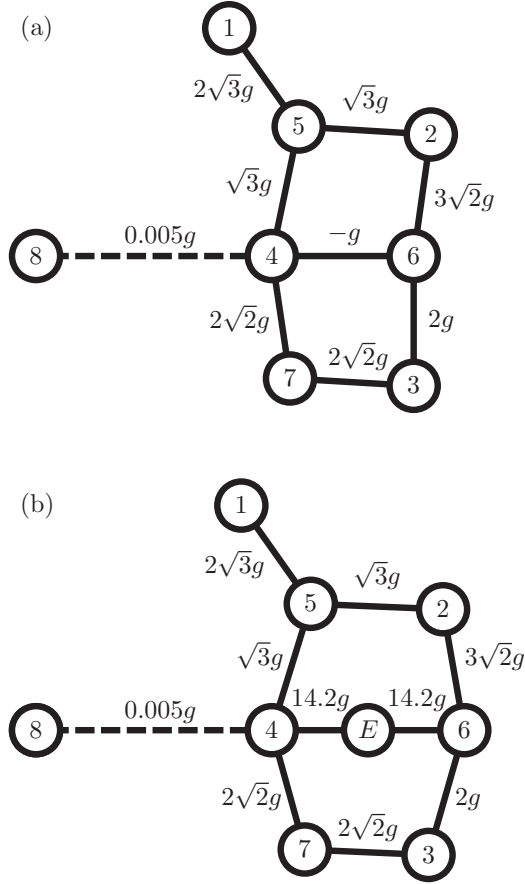


FIG. 2. Sketch of (a) the square-root Cholesky lattice associated to a four-element necklace (note the negative coupling), and (b) its nine-waveguide realization; see text for more details.

of the system parameters $\{\epsilon, g\}$. Its associated Cholesky matrix,

$$\mathbf{A} = \begin{pmatrix} \sqrt{\epsilon} & 0 & 0 & 0 \\ \frac{g}{\sqrt{\epsilon}} & \sqrt{\frac{\epsilon^2 - g^2}{\epsilon}} & 0 & 0 \\ 0 & g\sqrt{\frac{\epsilon}{\epsilon^2 - g^2}} & \sqrt{\frac{\epsilon(\epsilon^2 - 2g^2)}{\epsilon^2 - g^2}} & 0 \\ \frac{g}{\sqrt{\epsilon}} & \frac{-g^2}{\sqrt{\epsilon(\epsilon^2 - g^2)}} & \frac{g\epsilon^2}{\sqrt{2g^4\epsilon - 3g^2\epsilon^3 + \epsilon^5}} & \sqrt{\frac{\epsilon(\epsilon^2 - 4g^2)}{\epsilon^2 - 2g^2}} \end{pmatrix}, \quad (27)$$

has one negative element. This is not an issue as it is possible to falsify negative couplings using additional elements [37].

Our square-root lattice requires an array of eight coupled waveguides with one negative coupling [Fig. 2(a)]. We falsify it using nine waveguides [Fig. 2(b)] that share an effective core radius $r = 4.5 \mu\text{m}$ and cladding material with a refractive index $n_{\text{cl}} = 1.444$ as before. In order to falsify the negative coupling provided by Cholesky decomposition, we add an auxiliary value and optimize its refractive index and those of sites four and six to obtain $n_E = 1.448094$ and $n_4 = n_6 = 1.447901$. The rest of the cores share the index $n_i = 1.447900$ with $i = 1, 2, 3, 5, 7, 8$. The distances d_{ij} between the i th and j th waveguides are $\{d_{15}, d_{25}, d_{26}, d_{36}, d_{37}, d_{45}, d_{47}, d_{4E}, d_{6E}, d_{18}\} = \{5.00224, 5.5, 5.10528, 5.39646, 5.14751, 5.5, 5.14751, 4, 4, 9.79616\} r$

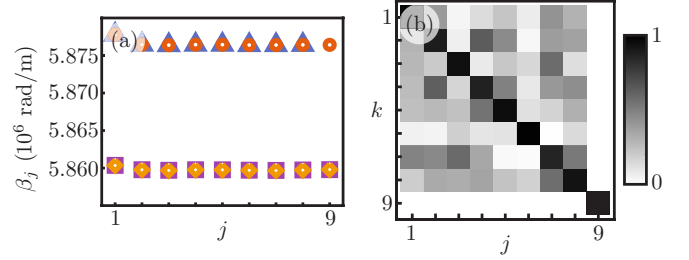


FIG. 3. (a) Propagation constant β_j obtained from the analytic Cholesky square-root array with negative coupling strength (triangles), its analytic nine-waveguide realization (circles), and its finite-element model simulation using COMSOL (diamonds) and our in-house *Mathematica* routines (squares). (b) Fidelity overlap between analytic and numerical normal modes, $\mathcal{F}_{j,k} = |\mathbf{a}_j^* \cdot \mathbf{n}_k|$.

with corresponding coupling strengths $\{g_{15}, g_{25}, g_{26}, g_{36}, g_{37}, g_{45}, g_{47}, g_{4E}, g_{6E}, g_{18}\} = \{24.1136, 12.0568, 20.883, 13.922, 19.6887, 12.0568, 19.6887, 98.8544, 98.8544, 0.0341018\}$ rad/m. These parameters are within experimentally reported values [33,36] and allow us to falsify the required coupled-mode matrix.

Figure 3(a) compares the propagation constants obtained from the eight-waveguide array with a negative coupling provided by the analytic Cholesky factorization in triangles, its nine-waveguide array realization where all coupling strengths are positive in circles, the numeric result from finite-element modeling using COMSOL in diamonds, and those produced by our in-house *Mathematica* routines in squares. The average relative error between the coupled-mode theory analytic results for the nine- and eight-waveguide arrays is of the order of $(3.747 \pm 8.570) \times 10^{-5}\%$ while that between COMSOL and analytic results is of the order $(2.855 \pm 0.044) \times 10^{-1}\%$. The relative error between COMSOL and our *Mathematica* results is of the order $(3.33 \pm 4.83) \times 10^{-3}\%$. In addition, we use the fidelity overlap,

$$\mathcal{F} = |\mathbf{a}_j^* \cdot \mathbf{n}_j|, \quad (28)$$

to compare the analytic \mathbf{a}_j and numeric \mathbf{n}_j normal modes of the nine-waveguide realization in Fig. 3(b). A fidelity value of one points to identical vectors, while a zero value to orthogonal vectors. The mean average value for the fidelities in our example is 0.913 ± 0.059 , which points to good agreement that can be improved between our analytic and finite-element models. We want to emphasize that the lowest fidelities arise from the two pairs of normal modes with a shared effective propagation constant. This points to the fact that it may be possible to construct a linear superposition for each of these pairs that has a better overlap with the closed-form analytic modes.

IV. FORCING ZERO-ENERGY MODES

It is straightforward to realize that the limit case,

$$\epsilon \rightarrow \beta_0 - \beta_{\text{min}}, \quad (29)$$

forces a pseudo-zero-energy mode in the mode-coupling matrix partner. Doing so invalidates the Cholesky decomposition SUSY results as the reduced mode-coupling matrix arising

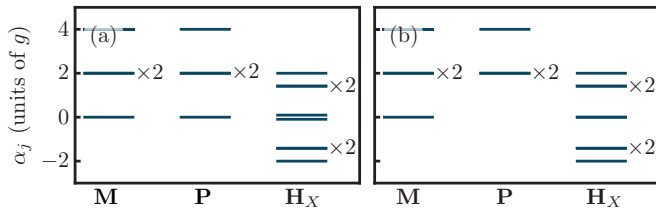


FIG. 4. Propagation constant α_j for the effective matrix $\mathbf{M}(\epsilon, g)$, its partner \mathbf{P} , and its Cholesky square-root array \mathbf{H}_X for (a) broken SUSY, $\epsilon > 0$, and (b) forcing a pseudo-zero-energy mode, $\epsilon = 0$.

from this choice is not positive definite. Still, the Cholesky lower \mathbf{A} and upper \mathbf{A}^\dagger triangular pair reconstructs the original coupled-mode matrix \mathbf{M} and provides a partner \mathbf{P} that has two pseudo-zero-energy modes. One of these modes is an isolated localized mode uncoupled to the array and the other is a normal mode of the array. However, the algebraic properties that sustain the SUSY analogy are not fulfilled; for example, the intertwining relations are no longer valid.

As a practical example, let us discuss the Cholesky arrays for a four-waveguide necklace. The simplest way to force a pseudo-zero-energy mode is by choosing the decomposition parameter $\epsilon = 2g$ [13]. This produces a null fourth column in the Cholesky matrix \mathbf{A} . Physically, this means that the SUSY partner is a three-waveguide array that has identical normal modes to the original mode-coupling matrix but for the one corresponding to the lowest propagation constant; compare the first two columns in Figs. 4(a) and 4(b). In the square-root lattice, this means that the eighth waveguide decouples from the fourth waveguide [Fig. 2(b)]. Thus, instead of the original broken SUSY without a pseudo-zero-energy mode [the third column in Fig. 4(a)], we do not account for the mode localized in the decoupled waveguide and obtain a spectrum with a null effective propagation parameter mode [the third column in Fig. 4(b)]. Formally, the arrays constructed in this manner do not fulfill SUSY QM. For example, the pseudo-zero-energy

mode does not arise from SUSY considerations but for the fact that we have an effective odd-dimensional, real symmetric, traceless mode-coupling matrix. Nevertheless, this pseudo-zero-energy mode is a normal mode of a pseudochirality operator that induces a π phase on the fields inside the first half of the waveguides and leaves the rest unchanged and may be used to design robust lasers [13,38,39].

V. CONCLUSION

We showed that Cholesky factorization is a reliable method to construct broken SUSY isospectral and square-root partners of photonic lattices described by coupled-mode theory. The mode-coupling matrices designed in this form fulfill all characteristics from SUSY QM with a Witten index two.

We constructed the isospectral and square-root partner of waveguide necklaces that may be experimentally realized using femtosecond laser-writing techniques. Broken SUSY square-root partners are interesting because negative coupling strengths arise for necklaces of dimension four or more. We used an additional waveguide to simulate such processes. A comparison of our analytic predictions with numeric finite-element model simulations shows good agreement in both cases.

It is possible to force a spectrum with a reduced range that points to exact SUSY using reduced mode-coupled matrices with a null main diagonal. Although these are not positive definite as required by Cholesky factorization, the resulting Cholesky matrices provide feasible partner photonic lattices. These partners do not correspond to exact SUSY as the intertwining relations are not fulfilled.

ACKNOWLEDGMENTS

B.M.R.-L. acknowledges fruitful discussions with B. Jaramillo Ávila and F. H. Maldonado Villamizar. P.I.M.B. thanks B. Jaramillo Ávila support with figure formatting.

-
- [1] S. M. Chumakov and K. B. Wolf, Supersymmetry in Helmholtz optics, *Phys. Lett. A* **193**, 51 (1994).
 - [2] M.-A. Miri, M. Heinrich, R. El-Ganainy, and D. N. Christodoulides, Supersymmetric Optical Structures, *Phys. Rev. Lett.* **110**, 233902 (2013).
 - [3] M.-A. Miri, M. Heinrich, D. N. Christodoulides, S. Nolte, S. Stutzer, and A. Szameit, Observation of supersymmetric scattering in photonic lattices, *Opt. Lett.* **39**, 6130 (2014).
 - [4] W. Walasik, B. Midya, N. M. Litchinitser, and L. Feng, Supersymmetry-guided method for mode selection and optimization in coupled systems, *Opt. Lett.* **43**, 3758 (2018).
 - [5] S. Longhi, Supersymmetric transparent optical intersections, *Opt. Lett.* **40**, 463 (2015).
 - [6] S. Longhi, Supersymmetric Bragg gratings, *J. Opt.* **17**, 045803 (2015).
 - [7] M. Heinrich, M.-A. Miri, S. Stutzer, R. El-Ganainy, S. Nolte, A. Szameit, and D. N. Christodoulides, Supersymmetric mode converters, *Nat. Commun.* **5**, 3698 (2014).
 - [8] M.-A. Miri, M. Heinrich, and D. N. Christodoulides, SUSY-inspired one-dimensional transformation optics, *Optica* **1**, 89 (2014).
 - [9] F. Cooper, A. Khare, and U. Sukhatme, Supersymmetry and quantum mechanics, *Phys. Rep.* **251**, 267 (1995).
 - [10] S. Longhi, Invisibility in non-Hermitian tight-binding lattices, *Phys. Rev. A* **82**, 032111 (2010).
 - [11] B. Midya, W. Walasik, N. M. Litchinitser, and L. Feng, Supercharge optical arrays, *Opt. Lett.* **43**, 4927 (2018).
 - [12] M. H. Teirmourpour, L. Ge, D. N. Christodoulides, and R. El-Ganainy, Non-Hermitian engineering of single mode two dimensional laser arrays, *Sci. Rep.* **6**, 33253 (2016).
 - [13] D. A. Smirnova, P. Padmanabhan, and D. Leykam, Parity anomaly laser, *Opt. Lett.* **44**, 1120 (2019).
 - [14] M. P. Hokmabadi, N. S. Nye, R. El-Ganainy, D. N. Christodoulides, and M. Khajavikhan, Supersymmetric laser arrays, *Science* **363**, 623 (2019).

- [15] B. Midya, H. Zhao, X. Qiao, P. Miao, W. Walasik, Z. Zhang, N. M. Litchinitser, and L. Feng, Supersymmetric microring laser arrays, *Photonics Res.* **7**, 363 (2019).
- [16] A. Zúñiga Segundo, B. M. Rodríguez-Lara, D. J. Fernández C., and H. M. Moya-Cessa, Jacobi photonic lattices and their SUSY partners, *Opt. Express* **22**, 987 (2014).
- [17] R. El-Ganainy, K. G. Makris, and D. N. Christodoulides, Local \mathcal{PT} invariance and supersymmetric parametric oscillators, *Phys. Rev. A* **86**, 033813 (2012).
- [18] R. El-Ganainy, L. Ge, M. Khajavikhan, and D. N. Christodoulides, Supersymmetric laser arrays, *Phys. Rev. A* **92**, 033818 (2015).
- [19] Q. Zhong, S. Nelson, M. Khajavikhan, D. N. Christodoulides, and R. El-Ganainy, Bosonic discrete supersymmetry for quasi-two-dimensional optical arrays, *Photonics Res.* **7**, 1240 (2019).
- [20] B. M. Rodríguez-Lara, R. El-Ganainy, and J. Guerrero, Symmetry in optics and photonics: A group theory approach, *Sci. Bull.* **63**, 244 (2018).
- [21] B. M. Rodríguez-Lara, Intensity-dependent quantum Rabi model: Spectrum, supersymmetric partner, and optical simulation, *J. Opt. Soc. Am. B* **31**, 1719 (2014).
- [22] M. H. Teimourpour, D. N. Christodoulides, and R. El-Ganainy, Optical revivals in nonuniform supersymmetric photonic arrays, *Opt. Lett.* **41**, 372 (2016).
- [23] P. Ramond, Dual theory for free fermions, *Phys. Rev. D* **3**, 2415 (1971).
- [24] A. Neveu and J. H. Schwarz, Factorizable dual model of pions, *Nucl. Phys. B* **31**, 86 (1971).
- [25] E. Witten, Dynamical breaking of supersymmetry, *Nucl. Phys. B* **188**, 513 (1981).
- [26] A. Lahiri, P. K. Roy, and B. Bagchi, Supersymmetry in quantum mechanics, *Int. J. Mod. Phys. A* **5**, 1383 (1990).
- [27] F. Cooper and B. Freedman, Aspects of supersymmetric quantum mechanics, *Ann. Phys.* **146**, 262 (1983).
- [28] S. Weinberg, *The Quantum Theory of Fields. Vol. 3: Supersymmetry* (Cambridge University Press, Cambridge, UK, 2005).
- [29] P. D. McIntyre and A. W. Snyder, Power transfer between optical fibers, *J. Opt. Soc. Am.* **63**, 1518 (1973).
- [30] B. Jaramillo Ávila, J. Naya Hernández, S. M. Toxqui Rodríguez, and B. M. Rodríguez-Lara, Symmetric supermodes in cyclic multicore fibers, *OSA Continuum* **2**, 515 (2019).
- [31] K. M. Davis, K. Miura, N. Sugimoto, and K. Hirao, Writing waveguides in glass with a femtosecond laser, *Opt. Lett.* **21**, 1729 (1996).
- [32] L. Shah, A. Y. Arai, S. M. Eaton, and P. R. Herman, Waveguide writing in fused silica with a femtosecond fiber laser at 522 nm and 1 MHz repetition rate, *Opt. Express* **13**, 1999 (2005).
- [33] D. Blömer, A. Szameit, F. Dreisow, T. Schreiber, S. Nolte, and A. Tünnermann, Nonlinear refractive index of fs-laser-written waveguides in fused silica, *Opt. Express* **14**, 2151 (2006).
- [34] A. Szameit, D. Blömer, J. Burghoff, T. Pertsch, S. Nolte, and A. Tünnermann, Controlled nonlinearity in femtosecond laser written waveguides, *Proc. SPIE* **6108**, 279 (2006).
- [35] M. Heinrich, F. Dreisow, A. Szameit, J. Thomas, S. Döring, S. Nolte, A. Tünnermann, and A. Ancona, Evanescently coupled fs laser-written type II waveguide array in lithium niobate, *Proc. SPIE* **7203**, 63 (2009).
- [36] A. Szameit and S. Nolte, Discrete optics in femtosecond-laser-written photonic structures, *J. Phys. B: At., Mol. Opt. Phys.* **43**, 163001 (2010).
- [37] R. Keil, C. Poli, M. Heinrich, J. Arkininstall, G. Weihs, H. Schomerus, and A. Szameit, Universal Sign-Control of Coupling in Tight-Binding Lattices, *Phys. Rev. Lett.* **116**, 213901 (2016).
- [38] L. Ge, Symmetry-protected zero-mode laser with a tunable spatial profile, *Phys. Rev. A* **95**, 023812 (2017).
- [39] A. Padrón-Godínez, B. Jaramillo-Ávila, and B. M. Rodríguez-Lara, Lasing in para-Fermi class-B microring resonator arrays, *Phys. Rev. A* **102**, 023511 (2020).